Proc. Natl. Acad. Sci. USA
Vol. 85, pp. 6758–6762, September 1988
Cell Biology

Three-dimensional immunogold localization of α-actinin within the cytoskeletal networks of cultured cardiac muscle and nonmuscle cells

(immunoelectron microscopy/deep freeze-etching/contractile proteins/cytoskeleton/tissue culture)

YUJI ISOBE*, FRED D. WARNER†, AND LARRY F. LEMANSKI*‡

*Department of Anatomy and Cell Biology, State University of New York, Health Science Center at Syracuse, Syracuse, NY 13210; and †Department of Biology, Syracuse University, Syracuse, NY 13210

Communicated by Keith R. Porter, May 9, 1988

ABSTRACT **The ultrastructural distribution of α-actinin was studied in cultured hamster heart cells by immunogold replica electron microscopy. This technique enabled us to localize α-actinin within the cytoskeletal networks at high resolution and in three dimensions. Colloidal gold, indicating the presence of α-actinin, was localized on the Z bands of nascent myofibrils in myocytes and on stress fiber bundles in nonmuscle cells. α-Actinin staining was also seen on stellate foci, where cytoskeletal filaments converged along the inner myocyte cell membranes. Intermediate filaments were associated with Z bands of myofibrils, stress fibers, and subplasmalemmal actin networks at the specific points where α-actinin was localized on these structures. Heavy meromyosin treatment prior to immunostaining confirmed that the thin filaments contained actin. These results suggest that α-actinin serves to interlink these various cytoskeletal elements. In addition, this protein may be involved in the initial phases of filament organization during myofibrillogenesis along the inner surface of the myocyte plasma membrane.**

In recent years, substantial progress has been made in the identification and localization of cytoskeletal proteins in muscle and nonmuscle cells. Immunofluorescence microscopy reveals that a number of these proteins have characteristic distribution patterns within different cytoplasmic domains of various cell types. Cytoskeletal proteins can be categorized into microfilament, intermediate filament, and microtubule systems. For each system, the component protein(s) such as actin, intermediate filament proteins, or tubulin can polymerize with various associated proteins to form specific filaments (1, 2).

α-Actinin has been studied extensively because it has a particularly interesting and unique distribution. In muscle, α-actinin is localized specifically at the Z bands, intercalated discs, and dense bodies, where it may have a role in anchoring actin filaments to other structures (3, 4). The detection of α-actinin in stress fibers and focal contact regions of nonmuscle cells suggests that the protein also may be involved in linking actin filaments to each other and to cell membranes (5). Previous studies dealing with α-actinin localization in cells *in vivo* (6, 7) and in culture (8–10), whether at the light or electron microscopic levels, have been based on two-dimensional images, while α-actinin molecules exist in complex three-dimensional cytoskeletal networks.

In the present study, we have examined the three-dimensional ultrastructural distributions of α-actinin in cardiomyocytes and nonmuscle cells in culture. This has been accomplished by combining freeze-drying and rotary replication methods on physically opened cells (11) with immunogold staining (10). This technique produces excellent ultrastructural preservation of the cell in three dimensions and reliable staining of specific proteins. The three-dimensional images presented here provide additional data concerning α-actinin distribution in the complex cytofilamentous network.

MATERIALS AND METHODS

Tissue Culture. Neonatal hamster heart cells were isolated, plated on glass coverslips in tissue culture dishes, and grown in Eagle's minimum essential medium with glutamine, antibiotics, and 15% fetal calf serum (12).

Physical Rupture of Cells. Living cultured cells were opened by using the "sandwich" method (11). Briefly, poly(L-lysine)-coated coverslips were placed on top of the cells and then peeled apart from the original coverslips in Hepes buffer at pH 7.0 (70 mM KCl/5 mM $MgCl_2$/3 mM EGTA/30 mM Hepes/10 μM Taxol/0.25 mM phenylmethylsulfonyl fluoride). Taxol was provided by the Drug Synthesis and Chemistry Branch, Division of Cancer Treatment, National Cancer Institute, Bethesda, MD.

Immunocytochemistry of α-Actinin and Tubulin and Heavy Meromyosin (HMM) Decoration of Actin. After physical rupture, the cells were washed twice in Hepes buffer, then incubated for 20–60 min at room temperature with a 1:30 dilution of rabbit anti-α-actinin antibodies prepared in our laboratory (13) or purchased commercially (Transformation Research, Framingham, MA). For negative controls, antibody absorbed with excess purified α-actinin or buffer alone was used instead of primary antibody. For positive controls, specimens were incubated with anti-tubulin antibody (Miles). The samples were washed three times with Hepes buffer, then incubated with a 1:4 dilution of goat anti-rabbit IgG coupled to 10- or 15-nm particles of colloidal gold (Janssen, Piscataway, NJ) for 30–180 min at room temperature. After three rinses in Hepes buffer, samples were fixed with 2% glutaraldehyde in the same buffer. For light microscopy, some gold-stained specimens were prepared by using silver enhancement (Janssen). The specimens for replica electron microscopy were further treated with 0.2% tannic acid for 30 min and finally with 0.5% OsO_4 for 30 min.

Some specimens were treated with HMM (Sigma) to label actin, prior to the primary antibody application.

Replica Preparation. Samples in 70% (vol/vol) ethanol as a volatile cryoprotectant were plunged into liquid-nitrogen-cooled Freon 13, then freeze-dried for 30–90 min at −90°C and rotary replicated with platinum at a shadowing angle of 20° and carbon at 90° in a Balzers BA 360M apparatus. After the coverslips were dissolved with hydrofluoric acid, the replicas were cleaned in bleach and picked up on 200-mesh

The publication costs of this article were defrayed in part by page charge payment. This article must therefore be hereby marked "*advertisement*" in accordance with 18 U.S.C. §1734 solely to indicate this fact.

Abbreviation: HMM, heavy meromyosin.

‡To whom reprint requests should be addressed.

Formvar/carbon-coated grids. Electron micrographs were taken with a Jeol 100CX-II electron microscope at 100 kV and were photographically reversed.

Immunoblotting. Antibody specificity was tested by immunoblotting. Samples of adult whole heart homogenates and tissue culture cell lysates were subjected to $NaDodSO_4$/PAGE (14). The proteins were transferred electrophoretically to nitrocellulose sheets and immunostained (15). Protein patterns were visualized by Coomassie blue staining on a duplicate gel.

RESULTS

The polyclonal antiserum against porcine skeletal muscle α-actinin was tested by immunoblotting. Fig. 1 illustrates the reaction of anti-α-actinin prepared in our laboratory on immunoblots. The antibody reacted specifically with a single band that has the same relative mobility as porcine skeletal muscle α-actinin. Similar results (not shown) were obtained by using an anti-α-actinin antibody purchased commercially. When used in silver-enhanced immunogold light microscopy, these antibodies stained those cytoskeletal domains known from immunofluorescent studies (5, 12, 16) to contain α-actinin (Fig. 2). Densely stained bands at regular intervals corresponded to the Z lines of organized myofibrils. Very slight staining was noted at some M lines; this observation requires more detailed analysis. A further concentration of labeling was seen as punctate patterns at the edges of cells and along filament bundles, which seemed to merge with myofibrils.

Staining specificity controls were performed by omitting primary antibody (Fig. 3*A*) or by using preabsorbed antibody (Fig. 3*B*) as negative controls and by using anti-tubulin antibody (Fig. 3*C*) as a positive control. Very slight background staining was detected on negative controls; microtubules stained heavily when the anti-tubulin immunogold procedure was used, with very little staining of other cytoskeletal elements.

We localized α-actinin in the cytoskeletal networks of muscle and nonmuscle cells in primary cultures. In the relatively loose cytoskeleton of fibroblast-like cells or in certain myocyte cytoskeletal domains that lacked extensive myofibril arrays, gold particles were mainly present on bundles of 7- to 10-nm filaments (Fig. 4). Individual filaments with diameters of 11–14 nm were often associated with the 7- to 10-nm filament bundles at sites of α-actinin labeling. We presume that these two types of filaments are actin and intermediate filaments, respectively, and that the bundles represent stress fibers, judged by their ability to bind HMM fragments (see below). Microtubules were distinguishable by their thick diameters (>22 nm).

Occasionally, in the cytoskeletal network on the inner face of the myocyte plasma membrane, actin and intermediate filaments appeared to radiate out from stellate filament foci that were labeled with anti-α-actinin-gold (Fig. 5). Some radiating filaments were aligned parallel into bundles. "Knobby" filaments, possibly myosin-containing filaments, were sometimes detected in association with the thin filament bundles (Figs. 5 and 6). In some instances similar thin filament bundles extended into thicker and more distinct myofibrils, which included many knobby filaments (Fig. 6). Some intermediate filaments extended between organized myofibrils and appeared to converge at the nascent Z band areas where gold had accumulated.

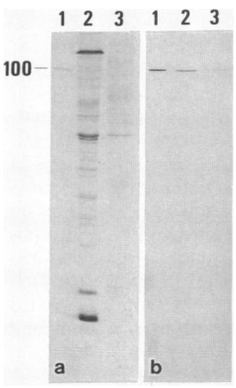

FIG. 1. Immunoblots of anti-α-actinin. (*a*) Coomassie blue-stained 10% polyacrylamide gel after electrophoresis in the presence of $NaDodSO_4$. (*b*) Immunoblots of proteins on nitrocellulose. Lanes: 1, purified porcine skeletal muscle α-actinin; 2, adult hamster heart homogenate; 3, neonatal hamster heart cell culture lysate. On the left is molecular mass in kDa.

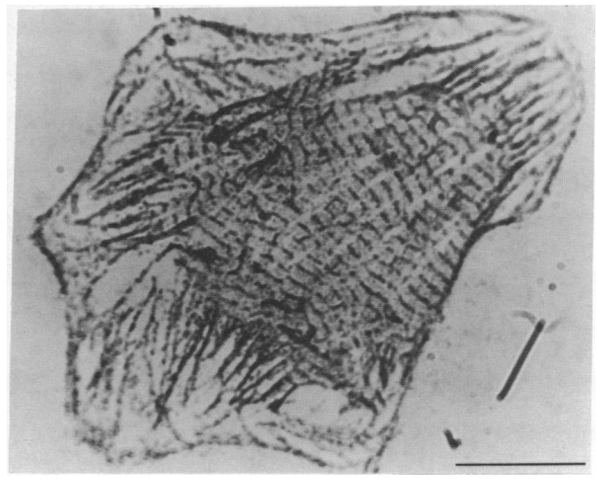

FIG. 2. Light micrograph of α-actinin-stained cardiac myocyte cultured for 3 days. The cell was physically opened, then incubated with rabbit anti-α-actinin and goat anti-rabbit IgG-coated colloidal gold particles; finally, the staining was enhanced with silver. Gold–silver deposits are localized on thin lines at regular intervals in the center of the cell and apparently correspond to myofibrillar Z lines. Note the staining in discrete striated patterns at the cell periphery. (×1700; bar represents 10 μm.)

To identify unequivocally the actin-containing filaments within such a complex network of cytoskeletal elements, we applied HMM prior to immunostaining for α-actinin. Actin-containing filaments, present in both myocytes and nonmuscle cells, reacted with HMM to produce the characteristic arrowhead decoration pattern along their entire lengths (Figs. 7 and 8). The extent of α-actinin labeling on HMM-decorated filaments was somewhat less than on specimens not treated with HMM. Most of the thin filaments in myofibrils and stress fibers were decorated with HMM and only a few gold particles were detectable on these filament bundles. However, anti-α-actinin labeling remained prominent at the intersections and/or contact sites of undecorated filaments (presumably intermediate filaments) with myofibrils and stress fibers (Fig. 7). Gold particles were also noted at intersecting points of undecorated filaments and individual actin filaments in the cortical network (Fig. 8).

Filaments 2–5 nm in diameter were observed occasionally in both cardiomyocytes and nonmuscle cells regardless of whether or not they were treated with antibodies and HMM. These filaments appeared to crosslink cytoskeletal filaments but did not decorate with HMM or stain with the antibodies we used (anti-α-actinin and anti-tubulin) (Figs. 4, 5, and 8).

DISCUSSION

The results demonstrate that indirect immunogold labeling combined with freeze-dry replica electron microscopy can be used to detect and localize α-actinin in cardiac muscle and nonmuscle cells at high resolution and in three dimensions. The specificity of the primary anti-α-actinin antibodies was shown by immunoblotting. Furthermore, as a screening method of immunostaining, we have taken advantage of

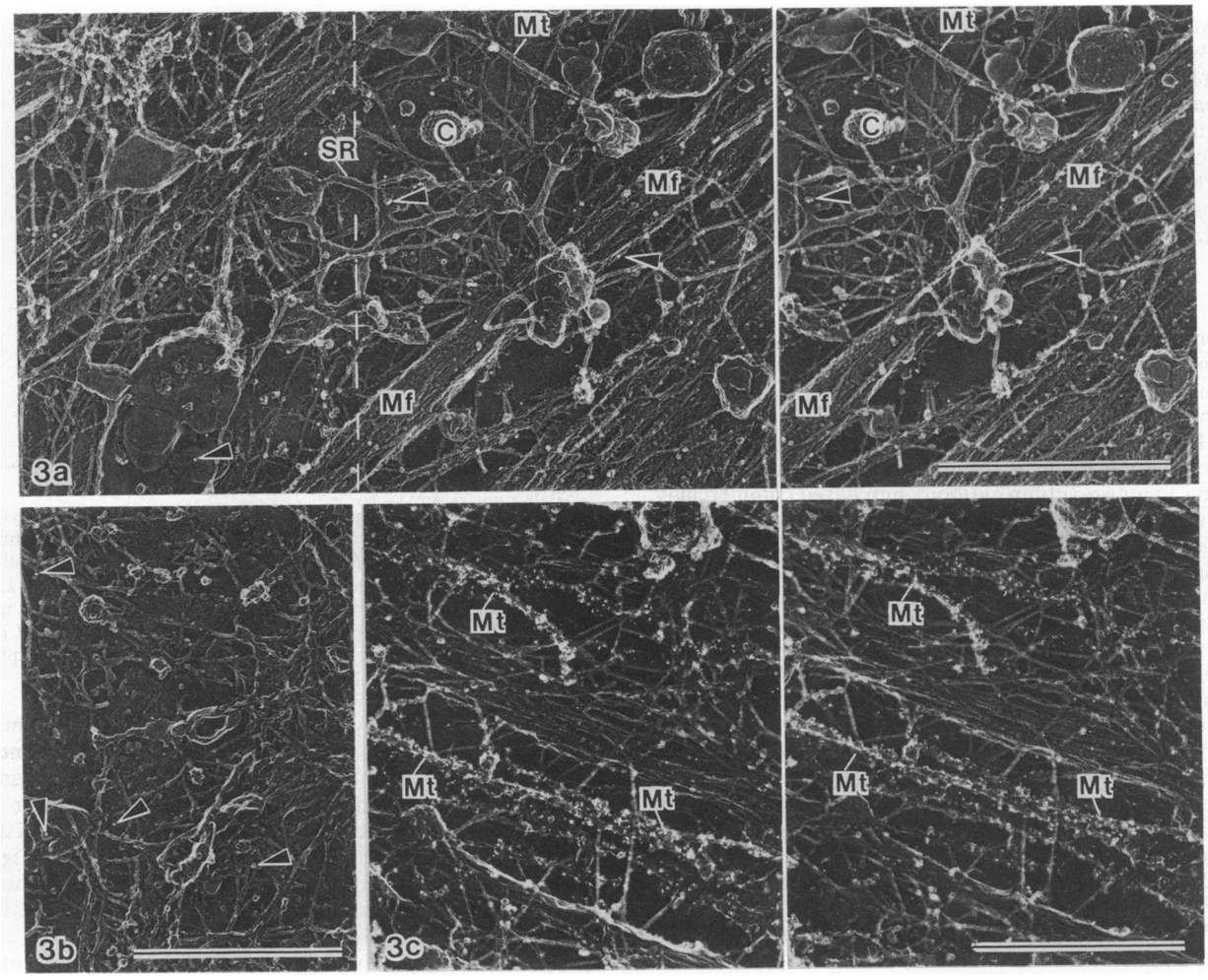

FIG. 3. Controls for immunogold labeling of 3-day-old cultured myocytes. The physically ruptured, freeze-etched, and replicated cells demonstrate the preservation of cytoskeletal and membranous structures after the labeling procedure. Goat anti-rabbit-IgG-conjugated 15-nm (*a*) or 10-nm (*b* and *c*) colloidal gold particles (seen as white spots) were used in these preparations as secondary probes. (*a*) Negative control omitting primary antibody. Everything to the right of the broken line is a stereopair. The nonspecific background staining is very low (arrowheads). Mf, nascent myofibrils; SR, sarcoplasmic reticulum; Mt, microtubule; C, clathrin-coated pit. (×32,000; bar represents 1 μm). (*b*) Negative control using preabsorbed anti-α-actinin antibody with excess antigen. Nonspecific staining is indicated by arrowheads. (×29,000; bar represents 1 μm.) (*c*) Positive control, shown in a stereopair. Anti-tubulin antibody was applied as a primary antibody. Only microtubules (Mt) are heavily decorated with gold particles. (×29,000; bar represents 1 μm.)

silver-enhanced immunogold light microscopy, which uses the same antibodies and the same immunostaining protocols as for replica electron microscopy. Light microscopic images of silver-enhanced gold deposits exhibit the overall α-actinin localization, which corresponds with previous data obtained by immunofluorescence microscopy (5, 12, 16) and microinjection techniques (17). These results corroborate the specificity and reliability of the present method in which nonspe-

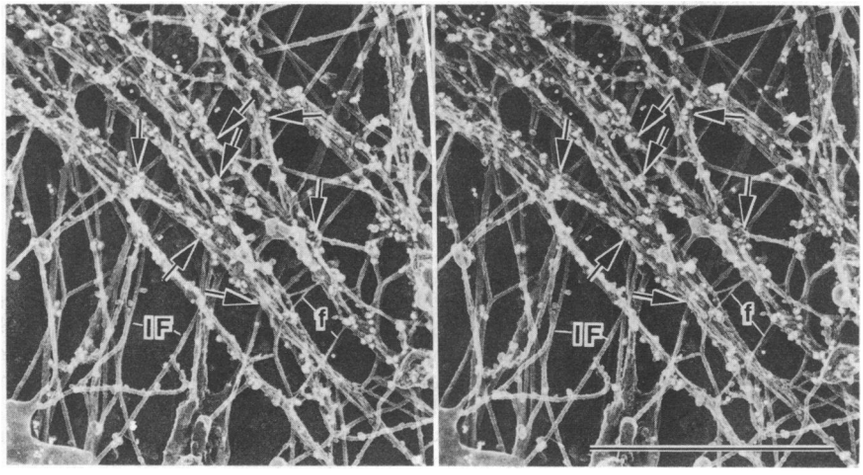

FIG. 4. Stereo replica electron micrographs demonstrate a cytoskeletal network of a fibroblastic cell from 3-day-old culture. The cell was physically opened, stained with anti-α-actinin, and tagged with 15-nm colloidal gold. Specimens in Figs. 4–6 were prepared by the same protocol. Gold particles are abundant on the filaments (diameter 7–10 nm in replicas) forming the bundles. Filaments 11–14 nm in diameter (IF) are often associated with the filament bundles at sites where α-actinin labeling has accumulated (arrows). f, 2- to 5-nm filaments. (×33,000; bar represents 1 μm).

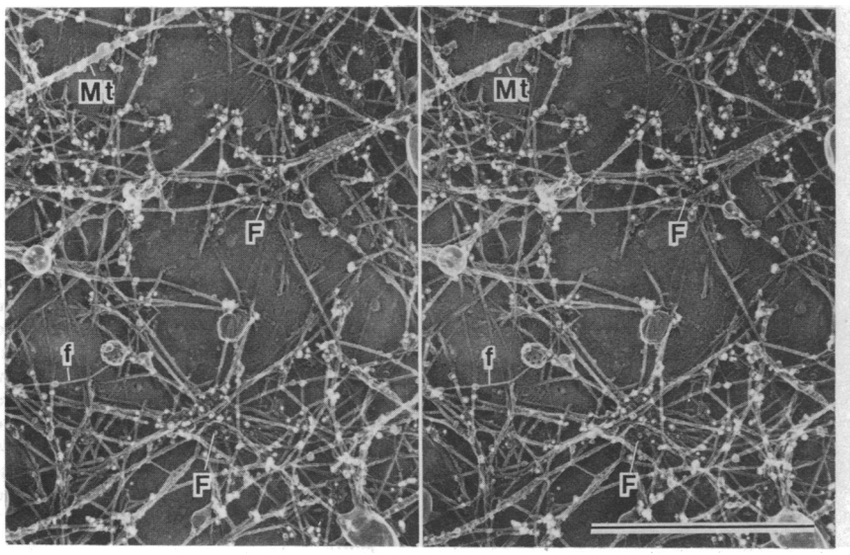

FIG. 5. Replica of a myocyte after 1 day in culture. Stereomicrographs exhibit a cytoskeletal network on the inner surface of sarcolemma comparable to that shown in Fig. 3*b*. Gold labeling shows that α-actinin accumulates where filaments converge as stellate foci (F). Note that small filament bundles extend into the filament foci. Mt, microtubule; f, 2- to 5-nm filaments. (×30,000; bar represents 1 μm.)

cific background staining is not significant even at the ultrastructural level.

One of the most interesting results from this study is the α-actinin localization at the stellate foci of filaments on the inner surface of the sarcolemma. These α-actinin-enriched foci are associated with small filament bundles and probably represent early Z bands of forming myofibrils. Previous studies have shown that the earliest myofibrils form just beneath the cell membrane in both skeletal and cardiac muscle (18, 19). It has been suggested that the Z band or its precursor composed of electron-dense material might be associated with the plasma membrane early in myofibrillogenesis (19). Our previous findings on thin-sectioned specimens suggested that α-actinin, a major protein composing the Z bands, is localized at membrane–thin filament association points (7, 20). In the present three-dimensional immunoelectron microscopic study, the gold localization on nascent myofibril-associated filament foci supports this proposal.

HMM treatment prior to α-actinin labeling allows the unequivocal identification of actin filaments. This study clearly shows that α-actinin is localized at the specific association sites of various actin-containing structures such as myofibrils, stress fibers, and cortical networks with HMM-undecorated intermediate filaments. Although there is little biochemical or other evidence indicating that α-actinin has a direct affinity for intermediate filaments, Hubbard and Lazarides (21) have shown that actin and desmin copurify from smooth muscle; furthermore, the two proteins cosediment. Moreover, they found that during purification desmin was associated with α-actinin. Singer *et al.* (8) have demonstrated by thin-section immunoelectron microscopy of cultured fibroblasts that intermediate filaments enter and/or cross microfilament bundles precisely at the regions of α-actinin localization. In striated muscle, intermediate filaments surround and enter the α-actinin-rich Z bands, as seen by immunofluorescence (22) and thin-section immunoelectron microscopy (23). The present three-dimensional analysis of α-actinin distribution strongly suggests that α-actinin is involved in interlinking intermediate filaments and actin filaments.

Thin (2- to 5-nm) filaments that appear to cross-link various cytoskeletal elements have been reported in various types of

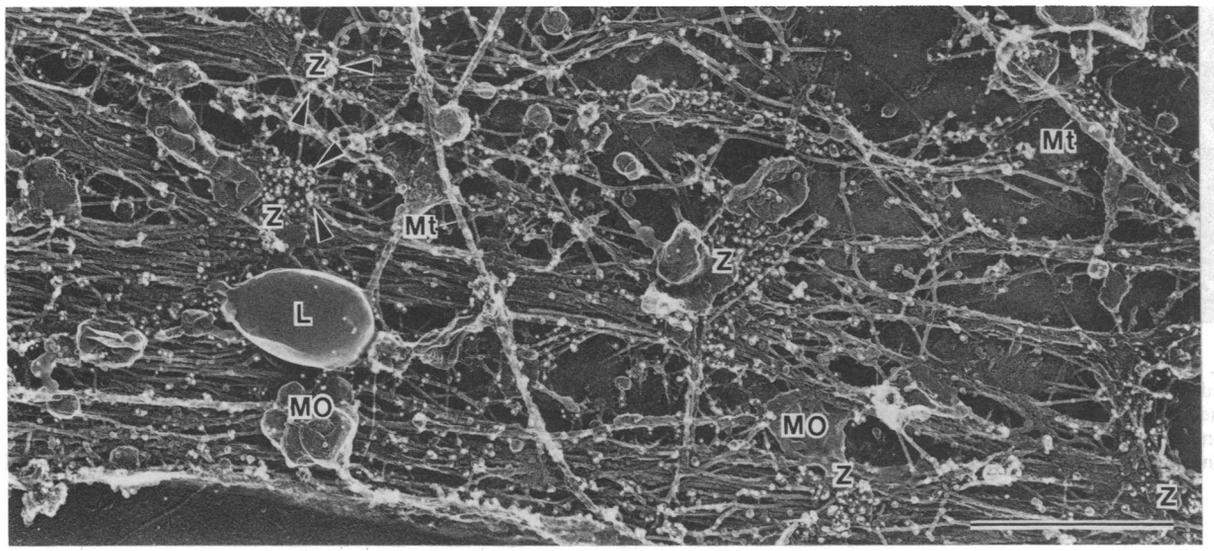

FIG. 6. Replica of a 3-day-cultured cardiac myocyte, showing a subsarcolemmal cytoskeletal network containing nascent myofibrils. Colloidal gold particles are mainly localized on or around the Z bands (Z) of myofibrils. Some filaments 11–14 nm in diameter and extended between myofibrils converge where gold particles accumulate on myofibrils (arrowheads). Mt, microtubules; MO, membranous organelles; L, lipid droplet. (×27,000; bar represents 1 μm.)

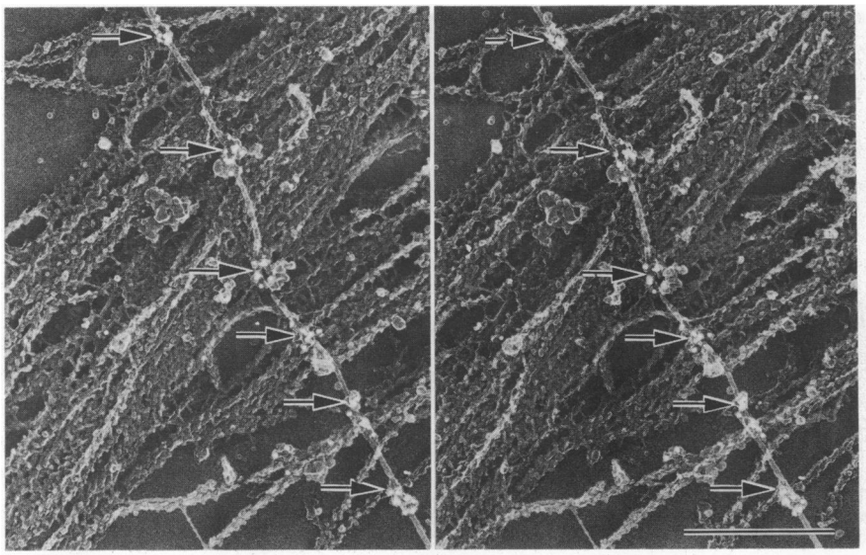

FIG. 7. Stereomicrograph showing a filament bundle from a 2-day-cultured nonmuscle cell. The cell was opened physically, treated with HMM, and incubated with rabbit anti-α-actinin serum and goat anti-rabbit IgG-coated 15-nm colloidal gold particles. Gold labels are localized at the points where an HMM undecorated intermediate filament is associated with an actin filament bundle (arrows). (×41,000; bar represents 0.5 μm.)

cells (2). α-Actinin has been considered a possible candidate protein for these filaments, since α-actinin is known to exist as a dimer having a diameter of 2–5 nm (24). However, our immunostaining results suggest that the 2- to 5-nm filaments do not contain α-actinin, at least in the two types of cultured hamster heart cells examined (myocytes and fibroblasts). Obviously, further work is required to define unequivocally the biochemical nature of these most interesting structures.

We thank Dr. D. E. Goll for his gift of purified α-actinin, Dori Cole, Cynthia Kaufman, Sharon Lemanski, Masako Nakatsugawa, and Joe Gromny for their technical assistance, and Nancy Snyder and Jo-Ann Pellett for typing the manuscript. Y.I. was supported, in part, by an American Heart Association New York Affiliate Postdoctoral Fellowship. The work was supported by National Institutes of Health Grant GM 20690 to F.D.W. and by National Institutes of Health Grants HL 32184 and HL 37702 and an American Heart Association grant to L.F.L.

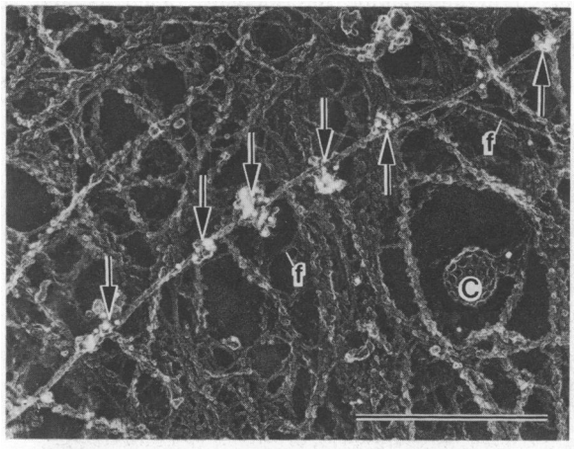

FIG. 8. Replica of a 2-day-cultured myocyte processed as in Fig. 7. Gold labels are localized at points where an HMM-undecorated intermediate filament is associated with HMM-decorated actin filaments of the cortical network. C, clathrin-coated pit; f, 2- to 5-nm filaments. (×51,000; bar represents 0.5 μm.)

1. Geiger, B. (1983) *Biochim. Biophys. Acta* **737,** 305–341.
2. Schliwa, M. (1986) *The Cytoskeleton* (Springer, New York), p. 5.
3. Goll, D. E., Suzuki, A., Temple, J. & Holmes, G. R. (1972) *J. Mol. Biol.* **67,** 469–488.
4. Schollmeyer, J. E., Furcht, L. T., Goll, D. E., Robson, R. M. & Stromer, M. H. (1976) in *Cell Motility,* eds. Goldman, R., Pollard, T. & Rosenbaum, J. (Cold Spring Harbor Lab., Cold Spring Harbor, NY), Vol. 3, pp. 361–388.
5. Lazarides, E. & Burridge, K. (1975) *Cell* **6,** 289–298.
6. Geiger, B., Dutton, A. H., Tokuyasu, K. T. & Singer, S. J. (1981) *J. Cell. Biol.* **91,** 614–628.
7. Lemanski, L. F., Paulson, D. J., Hill, C. G., Davis, L. A., Riles, L. C. & Lim, S.-S. (1985) *J. Histochem. Cytochem.* **33,** 515–522.
8. Singer, S. J., Ball, E. H., Geiger, B. & Chen, W.-T. (1982) *Cold Spring Harbor Symp. Quant. Biol.* **46,** 303–316.
9. Sanger, J. W., Sanger, J. M. & Jockusch, B. M. (1983) *J. Cell Biol.* **96,** 961–969.
10. Langanger, G., De May, J., Moeremans, M., Daneels, G., De Brabander, M. & Small, J. V. (1984) *J. Cell Biol.* **99,** 1324–1334.
11. Isobe, Y. & Shimada, Y. (1986) *Cell Tissue Res.* **244,** 47–56.
12. Lemanski, L. F. & Tu, Z.-H. (1983) *Dev. Biol.* **97,** 338–348.
13. Lemanski, L. F., Fuldner, R. A. & Paulson, D. J. (1980) *J. Embryol. Exp. Morphol.* **55,** 1–15.
14. Laemmli, U. K. (1970) *Nature (London)* **227,** 680–685.
15. Towbin, H., Staehelin, T. & Gordon, J. (1979) *Proc. Natl. Acad. Sci. USA* **76,** 4350–4354.
16. Dlugosz, A. A., Antin, P. B., Nachmias, V. T. & Holtzer, H. (1984) *J. Cell. Biol.* **99,** 2268–2278.
17. Sanger, J. M., Mittal, B., Pochapin, M. B. & Sanger, J. W. (1986) *J. Cell. Biol.* **102,** 2053–2066.
18. Fischman, D. A. (1972) in *The Structure and Function of Muscle,* ed. Bourne, G. H. (Academic, New York), Vol. 1, pp. 75–148.
19. Lemanski, L. F. (1973) *Am. J. Anat.* **136,** 487–526.
20. Hill, C. S. & Lemanski, L. F. (1985) *Eur. J. Cell Biol.* **39,** 300–312.
21. Hubbard, B. D. & Lazarides, E. (1979) *J. Cell Biol.* **80,** 166–182.
22. Lazarides, E. (1980) *Nature (London)* **283,** 249–256.
23. Tokuyasu, K. T., Maher, P. A. & Singer, S. J. (1985) *J. Cell. Biol.* **100,** 1157–1166.
24. Suzuki, A., Goll, D.E., Singh, I., Allen, R.E., Robson, R. M. & Stromer, M. H. (1976) *J. Biol. Chem.* **351,** 6860–6870.